SURFACE AND INTERFACE ANALYSIS, VOL. 26, 97–104 (1998)

Effects of Low-energy Electron Irradiation on Submonolayer Ammonia Adsorbed on Pt(111)

C. Bater, J. H. Campbell and J. H. Craig, Jr.*
Department of Physics, University of Texas at El Paso, 500 W. University Ave, El Paso, TX 79968-0515, USA

The effects of electron impact on ammonia-covered Pt(111) have been studied using temperature-programmed desorption (TPD) and electron-stimulated desorption (ESD). For coverages below one monolayer, ammonia adsorbs on the surface in two distinct TPD states: the α-state is broad and desorbs over the temperature range 150–350 K, and the β-state appears as a sharper peak at 150 K. The β-state was seen to be damaged by electron-beam impact much more readily than the α-state, resulting in the formation of atomically adsorbed N on the surface. The mass 28 recombinative nitrogen desorption TPD peak appearing at 550 K exhibited second-order desorption kinetics, further confirming the presence of atomically adsorbed nitrogen. The ESD kinetic energy distributions (KEDs) were obtained for $m/e = 1$ amu, which exhibited broad peaks generally. The H^+ KEDs were analyzed using empirical curve fits, with the resulting conclusion that the H^+ KEDs contain contributions from at least three different hydrogen-containing surface species. We believe that these three H^+ KED peaks are due to ESD from adsorbed NH_3, NH_2 and H. The ESD cross-section for NH_3 removal was measured in three different ways, all of which were found to be in general agreement, and which gave an averaged cross-section value of $Q_{tot} = 4 \times 10^{-17}$ cm². © **1998 John Wiley & Sons, Ltd.**

Surf. Interface Anal. **26**, 97–104 (1998)

KEYWORDS: ammonia; Pt; adsorption; electron irradiation

INTRODUCTION

The electron-stimulated dissociation of ammonia adsorbed on transition metal surfaces has been the subject of numerous investigations.[1–5] Using incident electrons to activate adsorbed molecules not only provides interesting insights into excited states, but may also serve as a non-thermal processing method. One of the possible ways to form a nitrogen adlayer on surfaces is to dissociate adsorbed ammonia, followed by removal of hydrogen from the surface. Several investigations of electron-stimulated dissociation of adsorbed ammonia on Pt(111) have been reported recently.[6–8] In early work done by Gland, electron beam-assisted adsorption of ammonia on Pt(111) at 200 K was observed.[5] Temperature-programmed desorption (TPD) data were used to show that ammonia adsorbed on Pt(111) was dissociated by electrons incident on the surface at 2000 eV. Although the states into which ammonia adsorbs at elevated temperatures are different from the states accessed at lower temperatures,[9,10] Gland did not investigate the effects of electron beam irradiation of ammonia at lower temperatures.[5] Burns *et al.* investigated electron-stimulated desorption (ESD) of ammonia adsorbed at 90 K, and found that molecular inversion of ammonia is one of the desorption mechanisms leading to desorption of neutral NH_3 species from the surface.[6] Burns *et al.* also measured threshold energies for various ESD channels and the neutral desorption cross-section, which was found to be 7×10^{-19} cm².[6] Stechel *et al.* detected gas-phase atomic hydrogen desorbing from the Pt(111) surface[7] during electron bombardment of NH_3/Pt(111). Recently, Sun *et al.*[8] conducted a high-resolution electron energy-loss spectroscopy (HREELS) study of electron-irradiated NH_3 overlayers on Pt(111) and found that NH_2(a) is the predominant decomposition product for temperatures below 200 K. Despite extensive studies, there are still several ambiguities regarding the ESD products from NH_3/Pt(111) and the electron-stimulated mechanisms producing them. In this work, we employ the TPD and ESD techniques to study electron-stimulated processes occurring at monolayer coverages and below for ammonia on Pt(111).

EXPERIMENTAL

All experiments were performed in a stainless-steel ultra high vacuum (UHV) chamber at base pressure 6×10^{-11} Torr. The chamber is equipped with a double-pass cylindrical mirror analyzer for x-ray photoelectron spectroscopy (XPS) and Auger electron spectroscopy (AES). The system also has two quadrupole mass spectrometers (QMS), one is used for residual gas analysis and TPD while the other is combined with a Bessel box energy analyzer[11] for electron-stimulated desorption experiments. A Kimball Physics low-energy electron gun provided incident electrons at 150 eV for the ESD experiments, which were incident on the surface at an angle of 70° off the surface normal.

* Correspondence to: J. H. Craig, Jr., Dept. of Physics, Univ. of Texas at El Paso, 500 W. University Ave., El Paso, TX 79968-0515, USA. E-mail: jcraig@utep.edu

CCC 0142–2421/98/020097–08 $17.50

Received 20 May 1997
Accepted 31 July 1997

The platinum crystal was spot-welded to a tantalum ribbon, which was resistively heated, and the sample was cooled by thermal contact with a liquid nitrogen reservoir. Temperature measurements were made with a chromel-alumel thermocouple spot-welded to the edge of the platinum crystal. Sample temperatures in the range 100–1500 K could be achieved.[12] The Pt crystal was initially cleaned by sputtering, followed by titration with oxygen. Contaminant oxygen and nitrogen were removed by heating the sample to 1300 K. Surface cleanliness was achieved when no carbon, oxygen or nitrogen peaks could be seen in the AES or XPS spectra. After the surface was clean, ammonia was dosed via a tubular-array molecular beam doser 0.5 cm in front of the crystal. Ammonia exposures were linear as a function of dosing time. The calibration of exposures is obtained by comparing our TPD spectra with those in the literature.[10] In our experiments, exposures of 0.25 L produced saturated α-NH_3 and exposures of 1.0 L produced the saturated $\alpha + \beta$ ammonia overlayer on Pt(111). This is in general agreement with the work of others.[7,9,10] A heating rate of 6 K s^{-1} was used in all TPD measurements reported here.

RESULTS

Temperature-programmed desorption studies of NH_3 on Pt(111)

Figure 1 shows the NH_3 TPD spectra for various exposures of Pt(111) to ammonia. Three distinct desorption states were observed at 110–120, 150 and 150–350 K. At low exposures (<0.25 L), a broad peak (α-state) appeared in the temperature range 250–350 K. The α-peak broadens significantly to low temperature as the ammonia exposures are increased, spanning the temperature range 150–350 K by 0.25 L. For exposures above 0.25 L, a second peak (the β-state) develops at 150 K, which saturates at 1 L. Compared to the α-peak, the β-peak is very sharp. The peak position of the β-peak does not change with respect to increasing ammonia exposure and is therefore believed to be due to first-order desorption of molecular ammonia. The physisorbed state (multilayer, ammonia ice) begins filling for exposures above 1 L and never saturates. The multilayer peak appears at 115 K. These TPD spectra are in qualitative agreement with the literature[9] for ammonia adsorption on Pt(111). In the experiments reported below, ammonia exposure was controlled such that only the α- and β-states were present during electron-irradiation and ESD experiments. Interesting electron-irradiation effects of ammonia multilayers on Pt(111) have been reported elsewhere.[13]

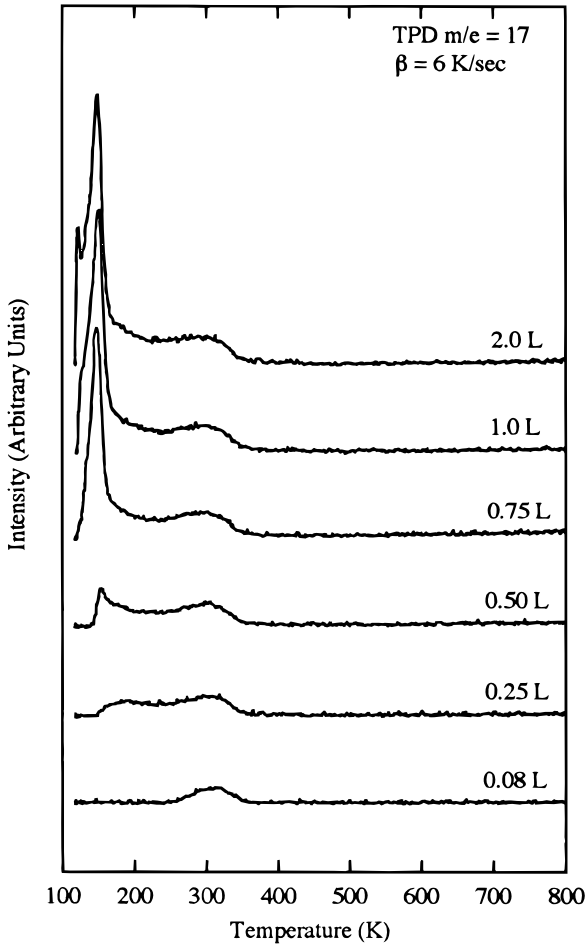

Figure 1. The TPD spectra from NH_3/Pt(111) for varying exposures of ammonia. The dosing temperature was 110 K.

Influence of electron irradiation on TPDs from NH_3/Pt(111)

The effects of electron irradiation of Pt(111) exposed to 1.0 L of ammonia or less was investigated using TPD. We report TPD of masses 14, 17 and 28 here, but note that masses 15 and 16 were also seen at low intensities. Figure 2(a) shows $m/e = 17$ TPDs obtained after the Pt(111) surface had been exposed to 1.0 L of ammonia and then irradiated with electrons (15 $\mu A\ cm^{-2}$) for 0, 2, 3, 5, 8 and 10 min. Initially, the β-peak is most strongly effected, and decreases rapidly with increasing electron-beam exposure. Two new peaks appear, one at 180 K and the other at 400 K; both peaks are analyzed in the discussion section below. In the early stages of electron irradiation, it is primarily the β-state that undergoes change. The only change seen in the α-peak during the early stages of electron-beam irradiation is a decrease in the high-temperature shoulder. However, after 2–3 min of electron irradiation, the β-peak has been substantially reduced and the shape of the lower temperature portion of the α-peak begins to change. Nevertheless, even after the highest electron doses used in this work, there is still some α- and β-ammonia present.

The total area under the $m/e = 17$ TPD traces is plotted in Fig. 2(b) as a function of electron beam dose. In the plot of Fig. 2(b), each point represents the total $m/e = 17$ peak area obtained following exposures of a virgin monolayer to the indicated electron dose at 150 eV. For these electron-irradiation damage studies, the electron beam was defocused so that the spatial dependence of the electron-beam current density is assumed to be negligible based on previously conducted electron-beam current density profiles. Thus, the ammonia population $N(t)$ is expected to decay exponentially in

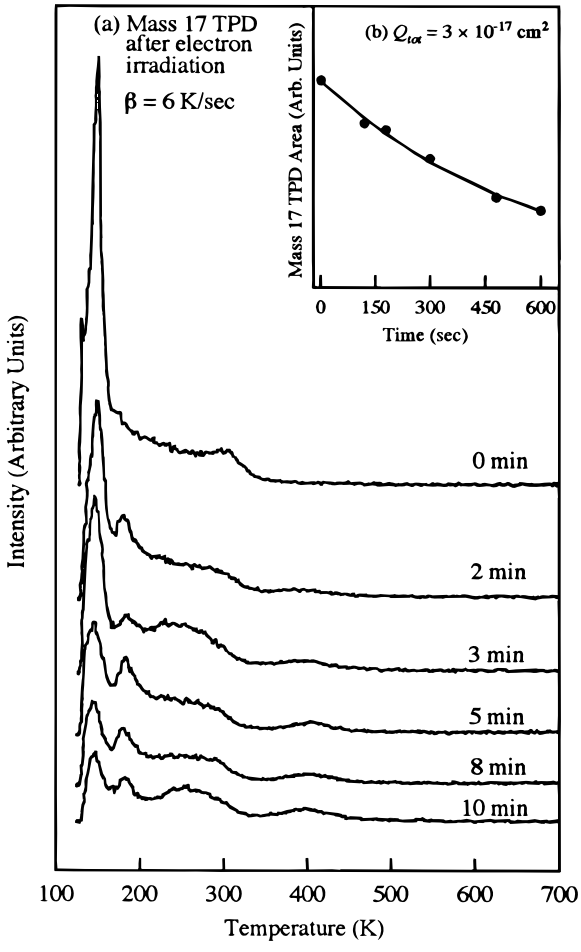

Figure 2. (a) Ammonia TPD spectra following electron irradiation at 15 μA cm^{-2} of adsorbed NH_3. Electron-beam exposure times are indicated in minutes for each curve, where 1 min = 4.7 × 10^{15} electrons cm^{-2}. Initial ammonia exposure was 1.0 L. (b) Plot of the loss of NH_3 *vs.* electron-beam exposure times. Ammonia loss calculated from the sum of the peak areas under the α- and β-peaks from the TPD in Fig. 2(a).

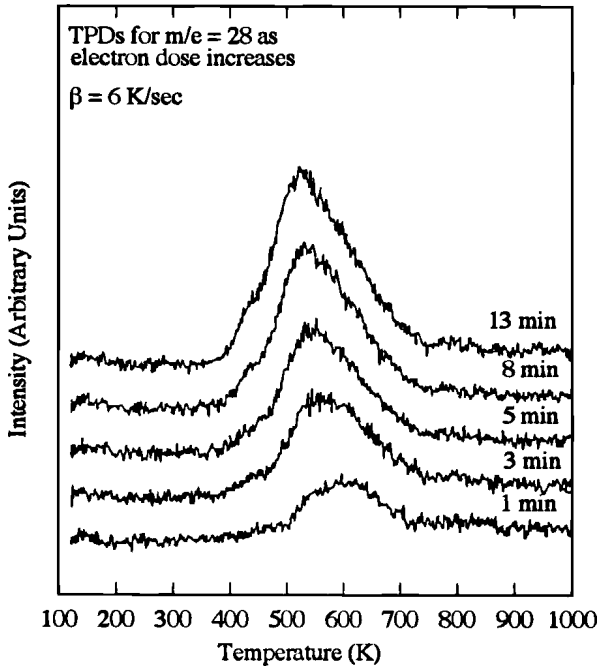

Figure 3. Temperature-programmed desorption for $m/e = 28$, reflecting the production of chemisorbed N atoms as electron-irradiation times of adsorbed ammonia increased, where 1 min = 4.7 × 10^{15} electrons cm^{-2}. Initial ammonia exposures and electron-beam current density were the same as in Fig. 2.

accordance with

$$N(t) = N_0 \exp(-JQt/e) \quad (1)$$

where N_0 is the initial ammonia surface concentration prior to electron-beam irradiation, Q is the total removal cross-section for ammonia by electron irradiation, J is the spatially and temporally constant current density, t is the time the overlayer was exposed to electrons and e is the elementary charge ($=1.6 \times 10^{-19}$ C). By fitting the curve in Fig. 2(b) to Eqn (1) using the decay constant $\beta = JQ/e$, a cross-section of $Q = 3 \times 10^{-17}$ cm^2 was obtained.

The TPDs obtained subsequent to monolayer and submonolayer ammonia doses on Pt(111) produce only small amounts of H_2 and N_2 as thermal desorption products. However, electron irradiation of such ammonia overlayers results in the observation of H_2 and N_2 thermal desorption peaks whose intensity increases with increasing electron-beam dose. Such behavior is demonstrated by the series of $m/e = 28$ TPD peaks shown in Fig. 3, where the $m/e = 28$ TPDs are plotted for electron doses of 1, 3, 5, 8 and 13 min. It can be seen that the $m/e = 28$ peak position moves to lower temperature as the electron dose increases or, equivalently, as the coverage of adsorbed nitrogen atoms increases. We therefore conclude that the $m/e = 28$ peak is due to diatomic nitrogen, which desorbs recombinatively. That the $m/e = 28$ peak is not due to desorbing CO was demonstrated by the fact that exposures of over 1 h to the system background resulted in negligible $m/e = 28$ TPD signals at 450–475 K,[12,14] where CO is normally seen desorbing from Pt(111). During a normal experiment, the maximum background exposure time following cleaning of the surface was 20 min. We also checked that the electron gun was not contaminated with or emitting CO, and that the dosing gas was not contaminated with CO. Thus, we conclude that the $m/e = 28$ TPD signal observed following electron-beam irradiation of ammonia on Pt(111) is due to recombinative desorption of atomic nitrogen as diatomic nitrogen. Desorption of molecular nitrogen is further confirmed by the observation of similar behavior in the mass 14 TPD near 550 K (see below), and by recent HREELS work showing that the Pt–N stretch intensity disappears after the surface is annealed above 500 K.[8]

The $m/e = 14$ TPDs show contributions from ammonia, ammonia fragments and fragments of diatomic nitrogen, and are shown in Fig. 4. Despite the variety of desorbates contributing to the $m/e = 14$ TPD signal, the TPD obtained from a clean Pt(111) surface dosed with 1.0 L of ammonia is very similar to the TPD obtained for $m/e = 17$, which suggests direct thermal desorption of molecular ammonia. Mass 15 and 16 were also observed displaying the same TPD behavior as mass 17. We attribute the similarity of the mass 14, 15, 16 and 17 TPDs to fragmentation of desorbing ammonia in the QMS ionizer. Exposure of ammonia adlayers on Pt(111) to electrons causes changes in the $m/e = 14$ TPD that parallel the changes seen in the

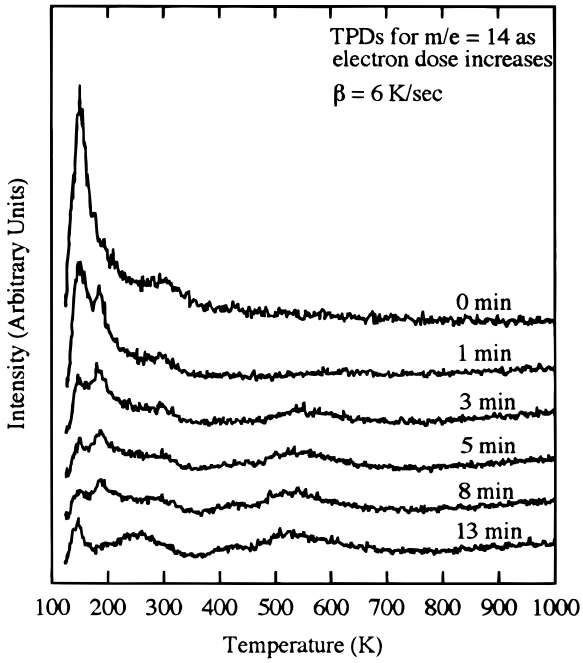

Figure 4. Temperature-programmed desorption for $m/e = 14$, confirming the 550 K peak in the $m/e = 28$ TPD to be recombinative N_2 desorption. The $m/e = 14$ TPD reflects thermal desorption of all nitrogen-containing species and exhibits intensity at 400 K (see text). The total electron fluence can be found from the relation 1 min = 4.7×10^{15} electrons cm^{-2}.

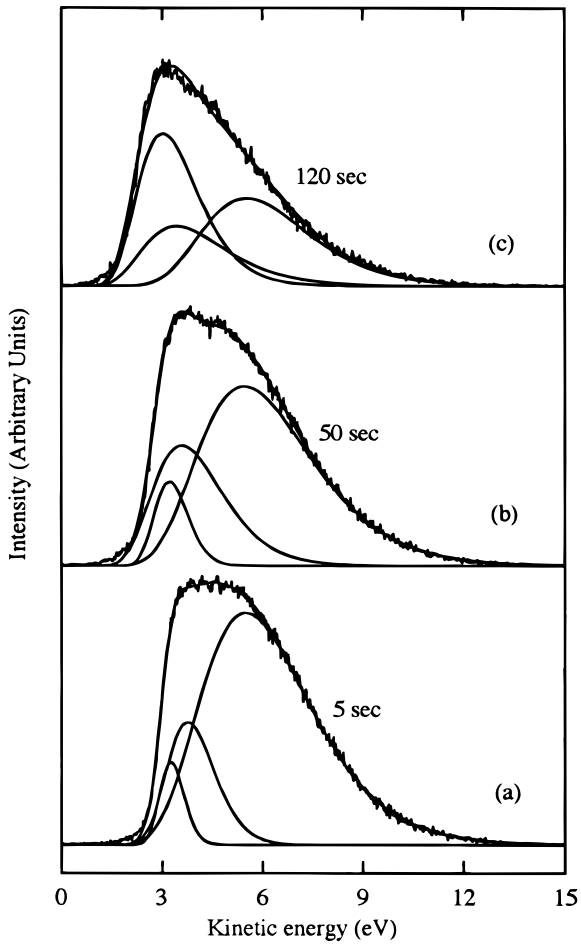

Figure 5. Time evolution of the H^+ KEDs from adsorbed ammonia on Pt(111) during electron irradiation. Each KED was obtained during a 5 s electron-beam exposure at 150 eV and 50 μA cm^{-2}. Total electron-beam exposure times are shown with each curve, where 50 s = 1.56×10^{16} electrons cm^{-2}. The component peaks are also shown; see text for details of the fitting procedure.

$m/e = 17$ TPDs following electron-beam exposure. The β-ammonia adsorbate state is depleted first, with a concomitant appearance of the desorbate state seen at 550 K. Once the β-state has been significantly removed, the α-state population decreases and the α-peak decreases in intensity. Further interpretations of the $m/e = 14$ TPD spectra will be presented in the discussion section.

Electron-stimulated desorption studies of NH_3/Pt(111)

Electron bombardment of ammonia on Pt(111) for exposures at and below 1.0 L was conducted so that its effects upon subsequent TPDs could be examined (previous section), so that ESD desorption products could be examined and so that surface intermediates, if present, could be detected and their structures and reactive properties might be inferred. In this section, we describe the ESD products observed during electron bombardment of NH_3/Pt(111), and analyze the H^+ ESD product ($m/e = 1$). In Fig. 5, three H^+ ESD kinetic energy distributions (KEDs) obtained at increasing electron-beam exposure times are shown, from which it is clear that electron irradiation of NH_3/Pt(111) produces strong H^+ ESD signals. Figure 5(a) was obtained with a 5 s electron-beam exposure at 50 μA cm^{-2}, Fig. 5(b) with 50 s and Fig. 5(c) with 120 s. As can be seen in Figs 5(a)–(c), the KED peak shape and position are strongly affected by electron-beam exposure time. For this reason, KED acquisition times had to be kept short so that the resulting KED peak shapes and positions best reflected the surface conditions being probed. Because KEDs are obtained by sweeping the Bessel box energy bandpass and accumulating the resulting QMS signal in multichannel scaler digital storage, KEDs acquired over times longer than 5 s have peak shapes and positions that are perturbed by their continuing electron-stimulated evolution. In this work, KEDs obtained in 5 s were found to have acceptable signal-to-noise levels, while at the same time exhibiting negligible electron-beam effects on KED peak shape.

From Figs 5(a)–(c), it is apparent that there are multiple states contributing to the H^+ KEDs obtained from NH_3-covered Pt(111) surfaces. Empirical fits to the experimental H^+ ESD KEDs, such as those in Fig. 5, lead to the conclusion that there are at least three hydrogen-containing surface states from which ESD of H^+ ions may occur. We will discuss the empirical curve fits and the model upon which they are based in the next section.

The N^+ ESD signals were considerably weaker than the H^+ signals, but the N^+ signals were strong enough so that KEDs could be obtained. Negative ESD ions

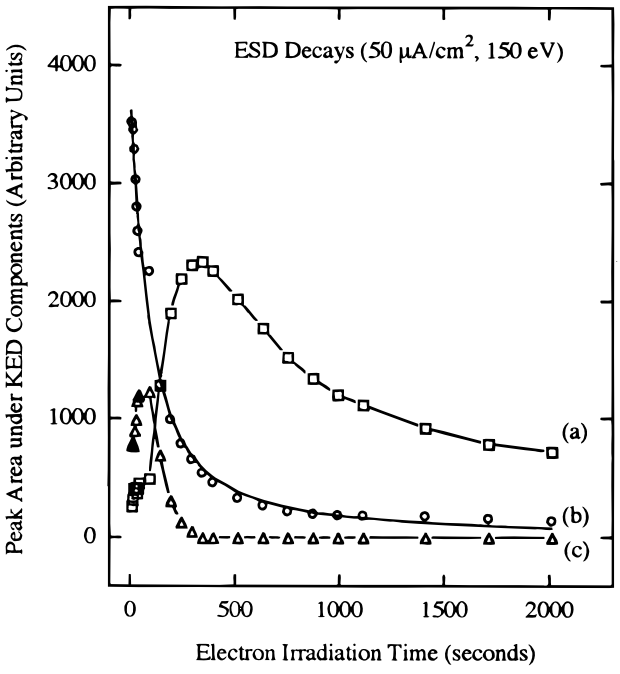

Figure 6. The H^+ decay curves obtained from the areas under each of the three peak components shown in Fig. 5 *vs.* electron-beam exposure times, where 50 s = 1.56×10^{16} electrons cm^{-2}. In the figure, curve (a) is the 4.0 eV KED peak, curve (b) is the 6.0 eV peak and curve (c) is the 3.3 eV peak. See text for details on the origins and interpretations of the curves. The total removal cross-section for NH_3 was calculated from the decay constant for the fitted curve to the data in curve (b).

were also investigated. An H^- ESD signal could be detected but no N^- signal was ever observed. For the purposes of this study, we note only that N^+ and H^- ESD signals can be detected and that KEDs for these

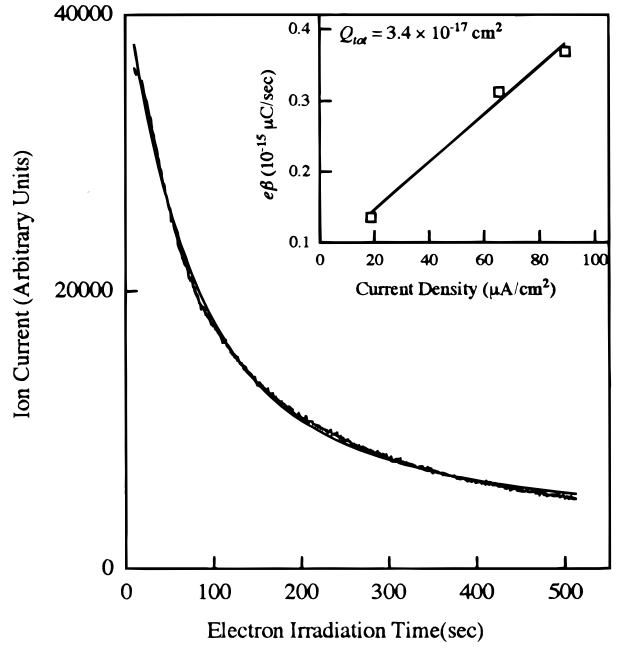

Figure 7. (a) Typical decay curve obtained at constant kinetic energy showing the decrease in the H^+ ESD signal from NH_3/Pt(111) as a function of electron-irradiation time, where 100 s = 3.15×10^{16} electrons cm^{-2}. (b) Plot of $e\beta$ *vs.* maximum current density, where β is the decay constant from decay curves such as the one in (a). The slope of this curve gives the total depletion cross-section for NH_3 from Pt(111): $Q_{tot} = 3 \times 10^{-17}$ cm^2.

ions can be obtained. Results from further analysis of these ESD ions and their KEDs will be presented in a forthcoming publication.

Curve-fitting of experimental KEDs

The KEDs were fitted to the sum of three theoretical KED curves by the least-squares method. The theoretical KED curves were based on a model utilizing one-dimensional potential energy surfaces originally proposed by Propst and Nishijima.[15] Because H^+ is of such a small mass, the reneutralization probability is low and the reneutralization factor could be ignored, resulting in theoretical KED curves with three adjustable parameters. The theoretical KED curve resulting from this model is

$$N(E) = \left(\frac{c_1}{E}\right)\exp\left[-c_2\left(\ln\frac{E}{E_0}\right)^2\right] \quad (2)$$

where $N(E)$ is the number of ions desorbing at kinetic energy E, and c_1, c_2 and E_0 are the three adjustable parameters. Fitting three theoretical KED curves to the experimental data requires nine adjustable parameters, which were reduced to six by the assumption that the peak positions were constant throughout the course of electron-beam irradiation and were equal to the peak positions obtained from a nine-parameter fit to the KED curve obtained at the lowest electron-beam exposure. By locking the three peak positions at 3.3, 4.0 and 6.0 eV, we were able to obtain excellent fits to the data over the entire range of electron doses used to obtain the KEDs.

The areas of each of the component KED curves obtained from a series of experimental KED curves obtained for increasing electron doses are plotted in Fig. 6. The 6.0 eV KED peak can be seen to decrease monotonically with increasing electron-beam exposure, the 4.0 eV KED peak increases initially before quickly decaying away and the 3.3 eV KED peak slowly increased in intensity up to 400 s electron-beam exposures, whereupon it slowly decreased.

Calculation of total ESD desorption cross-section

The ESD cross-section for the removal of NH_3 was obtained earlier by observing the electron beam-induced depletion of the $m/e = 17$ TPD signal, with the calculated cross-section being 3.0×10^{-17} cm^2. In this section, we calculate total NH_3 depletion cross-sections from two different ESD data sets.

First, we set the energy window of the Bessel box to 6 eV and monitored the H^+ ESD signal decay directly. Decays were taken at three different current densities and each was fitted to Eqn (3)[16]

$$I(t) = I_b + \alpha\left[\frac{1-\exp(-\beta t)}{\beta t}\right] \quad (3)$$

where $I(t)$ is the ion current at time t, β is the decay constant, I_b is the background signal and α is a fitted

amplitude parameter. Note that this equation was derived by assuming a non-uniform electron density in the spot illuminated by the electron beam at the surface.[16] Variations in electron-beam intensity have been shown experimentally to have a Gaussian profile for our system.[16] Assuming that the expression $e\beta = JQ$ holds true, i.e. that the decay constant is a linear function of current density, a plot of $e\beta$ *vs.* J will give a line of slope Q, which is the cross-section for the total removal of NH_3(a) by the electron beam, Q_{tot}. A plot of $e\beta$ *vs.* J for our data is shown in Fig. 7, from which $Q_{tot} = 3.4 \times 10^{-17}$ cm^2 is obtained for electron-beam removal of ammonia from Pt(111). The total ESD NH_3 removal cross-section was also obtained from the decay of the area of the 6.0 eV component of the fitted ESD KED curves as a function of increasing electron-beam exposure. This decay is plotted in Fig. 6 as curve b; a cross-section of $Q_{tot} = 6.4 \times 10^{-17}$ cm^2 was determined for the disappearance of ammonia by fitting Eqn (3) to the decay curve b in Fig. 6.

DISCUSSION

Electron-stimulated desorption products from NH_3/Pt(111)

Electron bombardment of a surface produces ionic and neutral desorbates, as well as adsorbed decomposition products. We discuss possible decomposition below. For ESD products, the problem is identification of the adsorbed states from which the desorbates originate. Typically, supporting analytical techniques must be used to fully characterize the surface.

In this work, we address only ionic ESD. As stated earlier, we see H^+, H^- and N^+ ESD ions from ammonia-covered Pt(111), with H^+ ions being the largest signal by far. Hydrogen has been observed to desorb from several ammonia-covered surfaces during electron bombardment,[4,17,18] including Pt(111).[6–8] The decomposition products that result from electron bombardment of ammonia-covered Pt(111) are not yet completely characterized. It has long been known[5] that ammonia does undergo electron-stimulated decomposition. An early EELS study did not have the resolution to discriminate between the adsorbed ammonia decomposition products.[10] A more recent HREELS study has confirmed the presence of NH_2(a) on the Pt(111) surface following electron bombardment.[8] Adsorbed molecules such as N_2H_2 and N_2H_4 as electron-induced surface products do not seem likely, based on both energetic and entropic arguments; additionally, no N–N-containing species were observed by HREELS.[8]

Based on the above arguments, we believe that the NH_2(a) species is the most prominent electron-beam decomposition product. The NH_2 species has been seen as an electron-induced decomposition product on other surfaces as well. Electron-induced NH_2(a) has been seen on Ni(110)[4] by ESDIAD, the presence of which was used to explain how electron bombardment caused the appearance of a high-temperature NH_3 desorption state, the γ-NH_3 state. The appearance of γ-NH_3 was believed to be due to a disproportionation reaction of the surface amido species at 500 K[4]

$$2NH_2(a) \rightarrow NH_3(g) + N(a) + H(a) \quad (4)$$

The NH_2(a) species was also proposed as an electron-irradiation intermediate for the NH_3/GaAs system, where it was also observed that electron-stimulated production of N(a) was much lower than for NH_x species ($x = 1, 2$).[18] Our data are in agreement with this latter observation, in that our $m/e = 28$ TPD peak (N_2) and our N^+ ESD signals were not large and grew slowly. Additionally, it seems reasonable that electron-induced multistep decomposition reactions would occur with lower probability than single-step processes. Our $m/e = 17$ and 14 amu TPD data (see Figs 2 and 4) also exhibit an electron-beam induced peak occurring at 400 K, which is very similar to the γ-NH_3 TPD peak observed from electron-irradiated Ni(110).[4] We attribute our high-temperature NH_3 TPD peak at 400 K as being due to the same disproportionation process proposed for Ni(110)[4] [i.e. Eqn (4)] or, possibly, due to the recombinative reaction between NH_2(a) and H(a)

$$NH_2(a) + H(a) \rightarrow NH_3(g) \quad (5)$$

Thus, it is clear that the predominant decomposition product of electron-irradiated NH_3(a) on Pt(111) at 100 K is NH_2(a).

We note that our modeling could as easily have been done with NH(a) as the surface intermediate rather than the NH_2(a) species, but the NH_2(a) species was chosen based on the reasoning described above. Our ESD KED work suggests (see below) that one of the two decomposition intermediates, NH(a) or NH_2(a), is present in very small amounts relative to the other. Danielson *et al.*[1] postulated the presence of NH(a) on Ru(0001) following electron irradiation, and the NH(a) species was detected on Ni(110) by EELS.[19] In fact, Bassignana *et al.*[19] reported that, because vibrational modes characteristic of NH(a) and NH_2(a) were absent at 500 K, the disproportionation reaction proposed by Klauber *et al.*[4] to explain desorption of γ-NH_3 could not be occurring, although they did not propose an alternative mechanism. For NH_3 on Pt(111), the recent HREELS study clearly demonstrated that NH_2(a) was present following electron irradiation at low surface temperatures, and that the characteristic NH_2(a) rocking and wagging vibrational modes were still present up to 200 K.[8] We note that our $m/e = 17$ TPD spectra exhibit a broad, low-intensity peak at 400 K following electron irradiation of the NH_3(a) overlayer, but this peak was not observed by Sun *et al.*[8] The appearance of the 400 K peak in our work may be associated with high surface defect or step densities. Nevertheless, our post-electron $m/e = 17$ TPD peak at 400 K suggests that some NH(a) or NH_2(a) species exist on the surface up to 400 K. We feel that NH_2(a) is the most likely precursor to ammonia desorption at 400 K, because NH(a) + 2H(a) and N(a) + 3H(a) are ternary and quaternary reactions, respectively.

The NH_2(a) electron-induced surface intermediate provides a clear rationalization of our apparent three-state ESD KEDs (see Fig. 5), where the three surface states from which H^+ ESD ions originate are NH_3(a),

NH_2(a) and H(a). The plots in Fig. 6 showing the behavior of the areas under the component curves that were summed to obtain the final fit to the H^+ ESD KED peaks also support the notion of NH_3(a), NH_2(a) and H(a) being the source states for H^+ ESD ions. As can be seen from Fig. 6, the 6.0 eV H^+ ESD component begins to decay immediately upon commencement of electron irradiation, and is therefore assigned as being due to NH_3(a). The 4.0 eV peak first increases, but quickly begins to decrease as electron irradiation continues. Because ammonia adsorbs molecularly on Pt(111), there is initially no NH_2(a) on the surface.[9,10] The H^+ intensity from this state would then be expected to rise during the initial stages of electron bombardment, followed by a decrease as the supply of NH_3(a) decreases. Thus, the 4.0 eV ESD KED peak is most reasonably assigned to ESD of H^+ from NH_2(a). Finally, the population of electron-induced H(a) via

$$NH_3(a) \rightarrow NH_2(a) + H(a) \quad (6)$$

or perhaps via Eqn (4) would, by the same arguments used in the case of the 4.0 eV peak, be expected to first increase, followed by a decrease as sources for H(a) are depleted by electron irradiation. The expected increase in the H^+ ESD intensity arising from NH_2(a) is seen because both Eqns (4) and (6) serve as sources for H(a); therefore, the 3.3 eV ESD KED peak is most likely to be due to ESD from H(a). Assigning the 3.3 eV component to H^+ ESD from H(a) is supported by our preliminary experimental observation that H^+ KEDs from H(a)/Pt(111) appear near 3.0 eV.

The TPD peak appearing at 180 K following electron irradiation is not as easily explained. Initially, we obtained large TPD peaks at 180 K, immediately leading to the suspicion that our ammonia dosing system was contaminated with water.[20] Indeed, this was in fact the case, so that examination of the $m/e = 18$ TPD, the O 1s XPS peak and the O(KLL) Auger peak all indicated the presence of water. However, even following rigorous cleaning procedures that resulted in the disappearance of the $m/e = 18$ TPD signal, the O 1s XPS peak and the O(KLL) Auger peak, there was still TPD peak intensity for both $m/e = 14$ and 17 amu at 180 K following electron irradiation of ammonia on Pt(111). The evidence described above indicates that we were successful in eliminating trace water contamination leading to the $m/e = 17$ TPD peak at 180 K, but that some other nitrogen-containing species exists on the surface following electron-beam irradiation of ammonia, and that this species produces a $m/e = 17$ TPD peak intensity at 180 K that is coincident with the water TPD peak. Possible explanations for the appearance of the 180 K TPD peak in both the mass 14 and 17 TPDs following electron irradiation will be explored further below.

It is well known that ammonia adsorbs molecularly in two states, each having distinct electronic structure[9] and TPD behavior,[5] and which saturate prior to the onset of multilayer growth.[10] The relationship of the β-NH_3 state to the α-NH_3 state has been described theoretically using slab and cluster calculations as being due to hydrogen-bonding effects.[21] In the theoretical description, β-NH_3 molecules donate $3a_1$ lone pair electron density to the hydrogens of a perpendicularly bound α-NH_3 molecule; the β-NH_3 molecule is tilted away from the surface normal by $69 \pm 5°$.[21] The driving force for the tilting action is an attractive interaction between the β-NH_3 hydrogens and the metal surface neighboring the α-NH_3, for which the local charge density has increased due to the presence of the electron-donating $3a_1$ orbital of the α-NH_3.[21] This picture of the structure and interactions of the α-NH_3 and β-NH_3 at saturation coverage provides reasonable explanations for observed TPDs,[5] photoelectron spectra[9] and EELS spectra[10] from ammonia-covered Pt(111). The recent theoretical description of NH_3/Pt(111) by Jennison *et al.* clearly rationalizes the bilayer–monolayer dichotomy[21] and provides a good description from which electron-irradiation effects of monolayer NH_3/Pt(111) can be understood.

Our data show a much stronger interaction of the incident electrons with the β-NH_3 relative to the α-NH_3, with the only significant change observable in the α-peak shape being the loss in the $m/e = 17$ TPD intensity in the high-temperature shoulder of the α-peak (see Fig. 2), the behavior of which is also seen in the $m/e = 14$ TPD (see Fig. 4). Additionally, the appearance of the 180 K TPD peak correlates with the disappearance of the high-temperature shoulder of the α-NH_3 state in the $m/e = 17$ and 14 TPDs, and the 180 K peak appears to stop growing once the α-peak high-temperature shoulder has been depleted to the maximum extent. Thus, we seem to see two processes occurring in the early stages of electron bombardment: removal of most of the β-NH_3 state, via desorption or decomposition; and removal and/or modification of some α-NH_3.

The large temperature range over which the α-NH_3 TPD peak is observed, i.e. 150–350 K, suggests a broad manifold of α-NH_3 adsorption states. Adsorption into the α-NH_3 state is known to be complete at 0.25 L;[9,21] as ammonia exposures increase, high-temperature α-NH_3 states fill first, followed by successively lower and lower temperature α-NH_3 states. This can be explained in one of two ways: a very heterogeneous surface or a coverage-dependent binding energy. Our Pt sample is a (111) crystal that has been carefully cleaned and annealed and, although we do not have LEED capability on this system, our Pt(111) sample exhibits TPD spectra in agreement with TPDs obtained elsewhere for Pt(111) surfaces checked by LEED.[5,8,9] Thus, we believe that surface imperfections and heterogeneous binding sites do not play a role in producing the widely observed α-NH_3 state. The broad nature of the α-state thus seems best described by a coverage-dependent binding energy for NH_3(a) on Pt(111). The observation that electron bombardment can cause depletion of the high-binding-energy sites without subsequent conversion of the lower-binding-energy to the higher-binding-energy form indicates that the activation barrier for conversion between various α-state species is high and that the coverage dependence of the α-NH_3 TPD desorption energy must be configuration dependent to some degree, most likely hydrogen bonding. Our experimental work, with rigorous exclusion of water, indicates that the TPD peak at 180 K seen for masses 14 and 17 is clearly due to NH_3 desorbing from an electron-induced state. Two possible sources for the 180 K TPD peak both involve the electron-induced decomposition product NH_2(a). Formation of NH_2(a) may result in

stronger hydrogen bonds to β-NH_3 molecules, resulting in an observed shift to higher temperatures for some β-NH_3 molecules. Another possible mechanism for the production of the states contributing to the 180 K TPD peak is recombinative desorption of ammonia via Eqn (5). Although 180 K seems to be too low a temperature for recombinative desorption of NH_3 ($E_A \sim 11$ kcal mol^{-1}), preliminary results obtained in our laboratory for co-adsorption of NH_3 and D_2 on Pt(111) following electron irradiation indicate NH_2D desorption at 180 K, suggesting that recombinative desorption of NH_3 may be occurring. Recombinative desorption of NH_3 at such a low temperature, if it is truly occurring, suggests that the NH_2 molecule may be activated or metastable. Regardless, the reaction mechanism producing the 180 K TPD peak is not straightforward. The ongoing co-adsorption experiments mentioned above may help to determine the origin of the 180 K TPD peak, and will be presented in a forthcoming publication.

Electron-stimulated desorption cross-sections

The three cross-section measurements reported above were averaged to obtain a total NH_3 ESD removal cross-section of $Q_{tot} \approx 4 \times 10^{-17}$ cm^2. Although we are not aware of any total removal cross-section measurements for NH_3/Pt(111), this value compares favorably with the cross-section of $Q_{tot} \sim 1.6 \times 10^{-16}$ cm^2 for removal of NH_3(a) from Ni(110),[4] $Q_{tot} \sim 6.3 \times 10^{-17}$ cm^2 for removal of NH_3(a) from GaAs(100),[18] and $Q_{diss} \sim 3 \times 10^{-16}$ cm^2 for the dissociation of NH_3/Rh(0001).[1] Compared to the neutral NH_3 desorption cross-section from Pt(111) of $Q_{neut} = 4 \times 10^{-19}$ cm^2,[22] our total removal cross-section indicates the primary result of electron-bombardment of ammonia on Pt(111) is ammonia decomposition.

SUMMARY AND CONCLUSIONS

We find that NH_3 adsorbs molecularly on the surface, as have others.[7–10] The effect of electrons incident on Pt(111) at 150 eV is primarily decomposition of the adsorbed ammonia. The total depletion cross-section for ammonia was determined in three different ways, and an average value for this cross-section was found to be $Q_{tot} = 4 \times 10^{-17}$ cm^2. Our TPD experiments indicate a molecular NH_3 species desorbing from the surface at 400 K. Desorption of NH_3 at 400 K strongly suggests the presence of NH_2(a) on the surface because desorption of NH_3 via reactions such as NH(a) + 2H(a) or N(a) + 3H(a) are lower probability ternary and quaternary reactions. After continued electron bombardment at 150 eV, nearly all of the hydrogen is removed from the Pt(111) surface and only atomically adsorbed nitrogen remains. Thus, irradiation of adsorbed ammonia at 150 eV is an effective means of obtaining N(a) on the Pt(111) surface.

Acknowledgements

The authors wish to thank J. M. White of the University of Texas at Austin for helpful comments regarding this work and manuscript.

REFERENCES

1. L. R. Danielson, M. J. Dresser, E. E. Donaldson and D. R. Sandstrom, *Surf. Sci.* **71**, 615 (1978).
2. C. W. Seabury, T. N. Rhodin, R. J. Purtell and R. P. Merrill, *Surf. Sci.* **93**, 117 (1980).
3. R. M. van Hardeveld, R. A. van Santen and J. W. Niemantsverdriet, *Surf. Sci.* **369**, 23 (1996).
4. C. Klauber, M. D. Alvey and J. T. Yates, Jr., *Surf. Sci.* **154**, 139 (1985).
5. J. L. Gland, *Surf. Sci.* **71**, 327 (1978).
6. A. R. Burns, E. B. Stetchel, D. R. Jennison and Y. S. Li, *J. Chem. Phys.* **101**, 6318 (1994).
7. E. B. Stechel, A. R. Burns and D. R. Jennison, *Surf. Sci.* **340**, 71 (1995).
8. Y.-M. Sun, D. Sloan, H. Ihm and J. M. White, *J. Vac. Sci. Technol. A* **14**, 1516 (1996).
9. G. B. Fisher, *Chem. Phys. Lett.* **79**, 452 (1981).
10. B. A. Sexton and G. E. Mitchell, *Surf. Sci.* **99**, 523 (1980).
11. J. H. Craig, Jr. and W. G. Durrer, *J. Vac. Sci. Technol. A* **7**, 3337 (1989).
12. J. H. Campbell, L. G. Gonzales, I. Ybarra and J. H. Craig, Jr., *Surf. Sci.* **306**, 204 (1994).
13. J. H. Campbell, C. Bater, W. G. Durrer and J. H. Craig, Jr., *Thin Solid Films* **295**, 8 (1997).
14. P. A. Thiel, E. D. Williams, J. T. Yates, Jr. and W. H. Weinberg, *Surf. Sci.* **84**, 54 (1979).
15. M. Nishijima and F. M. Propst, *Phys. Rev. B* **2**, 2368 (1970).
16. J. Lozano, J. H. Craig, Jr., J. H. Campbell and M. V. Ascherl, *Nucl. Instrum. Methods Phys. Res. B* **100**, 407 (1995).
17. F. P. Netzer and T. E. Madey, *Surf. Sci.* **119**, 422 (1982).
18. Y.-M. Sun, D. W. Sloan, T. Huett, J. M. White and J. G. Eckerdt, *Surf. Sci. Lett.* **295**, L982 (1993).
19. I. C. Bassignana, K. Wagemann, J. Küppers and G. Ertl, *Surf. Sci.* **175**, 22 (1986).
20. G. B. Fisher and J. L. Gland, *Surf. Sci.* **94**, 446 (1980).
21. D. R. Jennison, P. A. Schultz and M. P. Sears, *Surf. Sci.* **368**, 253 (1996).
22. A. R. Burns, D. R. Jennison and E. B. Stechel, *Phys. Rev. Lett.* **72**, 3895 (1994).

